Electronic Supplementary Material (ESI) for Inorganic Chemistry Frontiers.

Supporting Information for

Influence of the external magnetic field and magnetic-site dilution on the magnetization dynamics of a coordination network based on ferromagnetic coupled dinuclear dysprosium(III) units

Xuejing Zhang, Na Xu,* Wei Shi, Bing-Wu Wang, and Peng Cheng*

Table of Contents

1. Structure and Crystallographic Studies

Table S1 Selected crystallographic parameters, bond lengths and angles of **Dy**

	Dy
Formula	$C_{20}H_{22}Dy_2N_{12}O_{12}$
Fw	947.50
Temp, K	120(2)
Crystal syst	Monoclinic
Space group	$P2_1/c$
a, Å	9.72904(17)
b, Å	11.3592(2)
c, Å	24.6724(4)
α, deg	90
ß, deg	93.8572(17)
γ, deg	90
V, Å^3	2720.47(8)
Z	4
Dc, g/cm^3	2.3131
μ (mm^{-1})	5.539
Data/ parameter	4785 / 419
obs reflns	10756
θ range, (°)	5.84 - 50
R_{int}/GOF on F^2	0.0279 / 1.059
R_1, wR_2[I>2σ (I)]	0.0258, 0.0557
R_1, wR_2(all data)	0.0317, 0.0590
max/min, e Å^{-3}	0.60/-0.73

Dy			
Bonds/Angles	(Å / °)	Bonds/Angles	(Å / °)
Dy(1)-O(3)	2.232(3)	N(16)-Dy(1)-N(36)	148.58(11)
Dy(1)-O(14)	2.294(3)	O(42)-Dy(1)-Dy(2)	172.12(8)
Dy(1)-O(22)	2.384(3)	O(42)-Dy(1)-O(22)	70.82(10)
Dy(1)-O(42)	2.367(3)	O(42)-Dy(1)-N(16)	100.55(11)
Dy(1)-O(46)	2.387(3)	O(42)-Dy(1)-O(46)	76.22(11)
Dy(1)-O(32)	2.378(3)	O(42)-Dy(1)-O(32)	85.69(11)
Dy(1)-N(16)	2.578(4)	O(42)-Dy(1)-N(36)	62.45(11)
Dy(1)-N(36)	2.639(4)	O(46)-Dy(1)-Dy(2)	104.92(8)
Dy(2)-O(3)	2.308(3)	O(46)-Dy(1)-N(16)	71.26(11)
Dy(2)-O(11)	2.373(3)	O(46)-Dy(1)-N(36)	78.84(11)
Dy(2)-O(14)	2.221(3)	O(32)-Dy(1)-Dy(2)	90.03(8)
Dy(2)-O(33)	2.369(3)	O(32)-Dy(1)-N(16)	135.87(11)
Dy(2)-O(43)	2.397(3)	O(32)-Dy(1)-O(46)	150.54(10)
Dy(2)-O(45)	2.400(3)	O(32)-Dy(1)-N(36)	72.26(11)
Dy(2)-N(26)	2.611(4)	N(36)-Dy(1)-Dy(2)	109.92(8)
Dy(2)-N(5)	2.619(4)	O(3)-Dy(2)-Dy(1)	34.78(7)
O(3)-Dy(1)-Dy(2)	36.15(7)	O(3)-Dy(2)-O(11)	80.53(10)
O(3)-Dy(1)-O(14)	70.52(10)	O(3)-Dy(2)-O(33)	151.43(10)
O(3)-Dy(1)-O(22)	150.74(10)	O(3)-Dy(2)-N(5)	72.67(11)
O(3)-Dy(1)-N(16)	103.08(11)	O(3)-Dy(2)-O(45)	123.47(11)
O(3)-Dy(1)-O(42)	138.42(10)	O(3)-Dy(2)-N(26)	134.98(11)
O(3)-Dy(1)-O(46)	79.66(11)	O(33)-Dy(2)-Dy(1)	170.88(7)
O(3)-Dy(1)-O(32)	100.04(11)	O(33)-Dy(2)-O(11)	71.76(10)
O(3)-Dy(1)-N(36)	80.02(11)	O(33)-Dy(2)-O(43)	84.37(11)
O(14)-Dy(1)-Dy(2)	34.37(7)	O(33)-Dy(2)-N(5)	100.30(11)
O(14)-Dy(1)-O(22)	80.37(10)	O(33)-Dy(2)-O(45)	77.45(11)
O(14)-Dy(1)-N(16)	72.39(11)	O(33)-Dy(2)-N(26)	62.70(10)
O(14)-Dy(1)-O(42)	150.22(10)	O(43)-Dy(2)-Dy(1)	91.40(7)
O(14)-Dy(1)-O(46)	125.34(11)	O(43)-Dy(2)-N(5)	137.28(10)
O(14)-Dy(1)-O(32)	80.82(10)	O(43)-Dy(2)-O(45)	149.14(10)
O(14)-Dy(1)-N(36)	135.57(11)	O(43)-Dy(2)-N(26)	70.80(10)
O(22)-Dy(1)-N(16)	64.07(11)	N(5)-Dy(2)-Dy(1)	88.29(8)
O(22)-Dy(1)-O(46)	116.72(11)	O(45)-Dy(2)-Dy(1)	102.75(8)
O(22)-Dy(1)-N(36)	125.24(10)	O(45)-Dy(2)-N(5)	71.29(11)
N(16)-Dy(1)-Dy(2)	87.13(8)	O(45)-Dy(2)-N(26)	78.70(11)

Table S2 Selected examples of high-dimensional **Dy-MOFs** behaving as SMMs.

Structural formal	Structure dimensionality	DC field(Oe)	U_{eff}(K)	Hysteresis loop/Coercive field(Oe)	Magnetic interaction	Ref
$[Dy(3\text{-}py\text{-}4\ pmc)(C_2O_4)_{0.5}(OH)(H_2O)]$	2	0	186	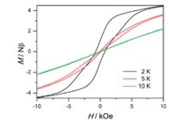 720 (2 K)	ferromagnetic	33
$[Ln(phen)\text{-}(L)]_n$	3	0	131	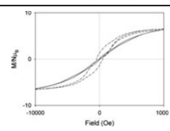	ferromagnetic	32
$Dy_2(INO)_4(NO_3)_2\cdot 2CH_3CN$	3	0	110		ferromagnetic	34
$[Dy_2(hmi)_2(NO_3)_2(MeOH)_2]_{\infty}\cdot MeCN$	2	700	71		ferromagnetic	29
$[Dy_2(apca)_4(\mu_2\text{-}OH)_2(H_2O)_2]_n$	2	0	59	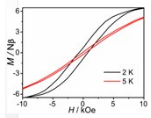 740 (2 K)	ferromagnetic	This work
$\{[Dy_2(FDA)_3(DMF)_2]\cdot 1.5DMF\}_n$ $[Dy_2(FDA)_3(DMF)_2(CH_3OH)]_n$	3	2000	41.8/67.5		ferromagnetic	37
$Dy(C_2O_4)_{1.5}(phen)]\cdot 0.5H_2O$	3	1200	35.5/32.6		ferromagnetic	36

3-py-4-pmc: 2-(3-pyridyl)pyrimidine-4-carboxylate; L: 5-hydroxyisophthalic acid; phen: 1, 10-phenanthroline; HINO = isonicotinic acid N-oxide; Hapca : 3-aminopyrazine-2-carboxylic acid; hmi: (isonicotino)hydrazine; H_2FDA = furan-2,5-dicarboxylic acid

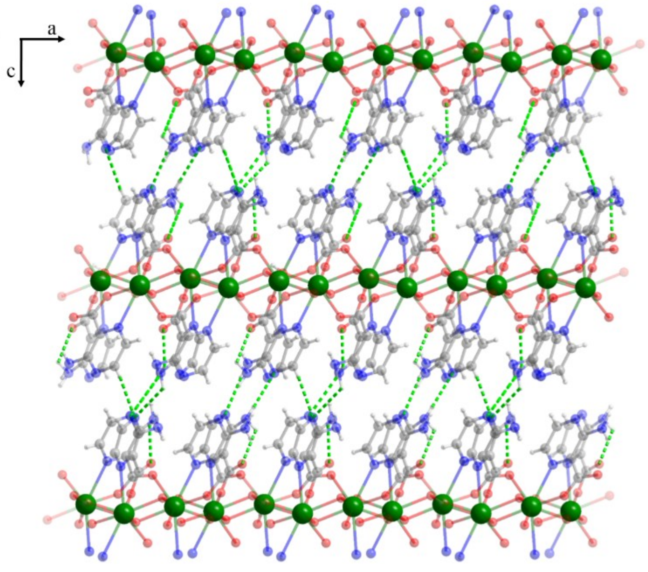

Figure S1 The supramolecular network of **Dy** connected by hydrogen bonds.

2. Powder X-ray Diffraction (PXRD) and Thermal analyses(TG)

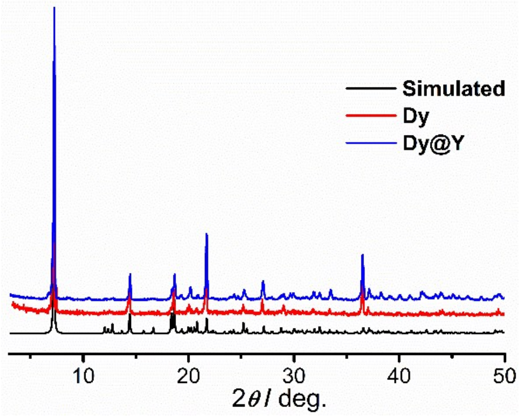

Figure S2 Simulated and measured PXRD of **Dy** and **Dy@Y**.

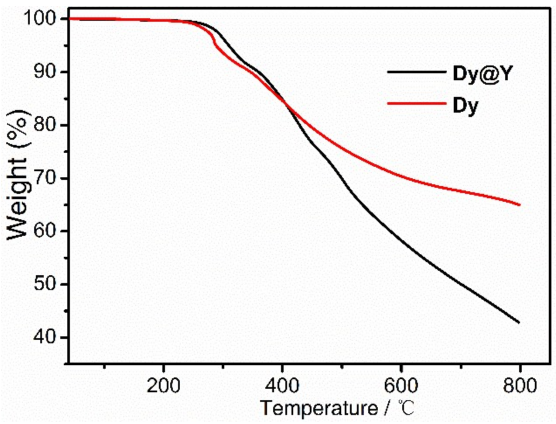

Figure S3 TGA of **Dy** and **Dy@Y**.

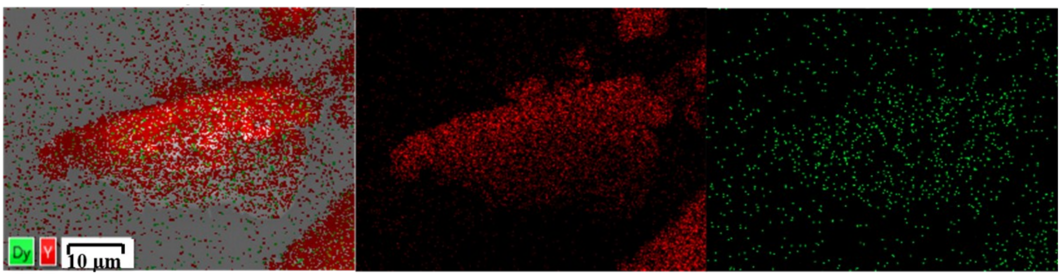

Figure S4 SEM image of **Dy@Y**.

3. Other Magnetic Data

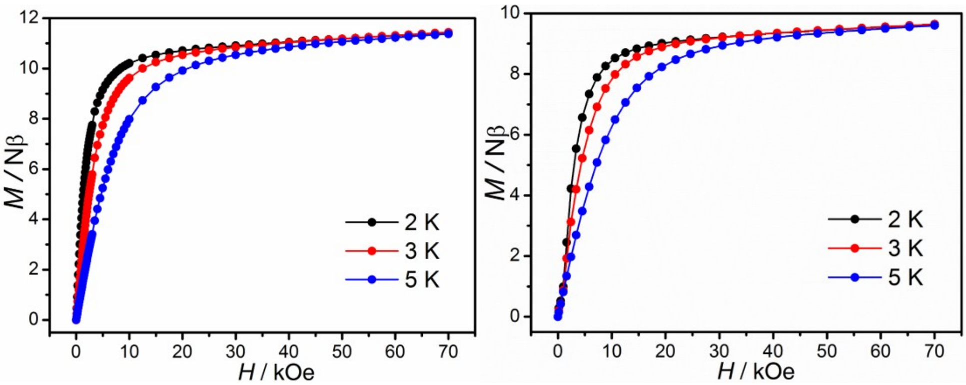

Figure S5 variable-field magnetizations of **Dy** (left) and **Dy@Y** (right).

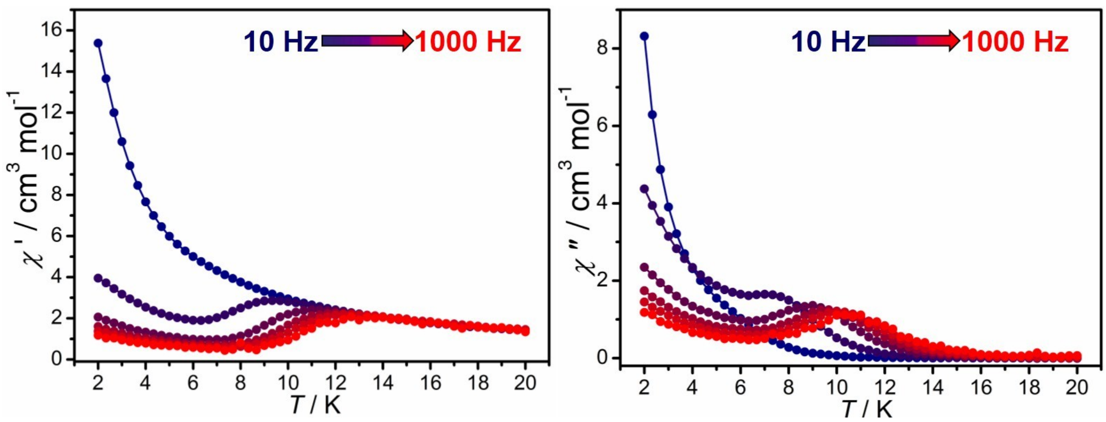

Figure S6 Temperature dependence of the ac susceptibilities of **Dy** under zero dc field.

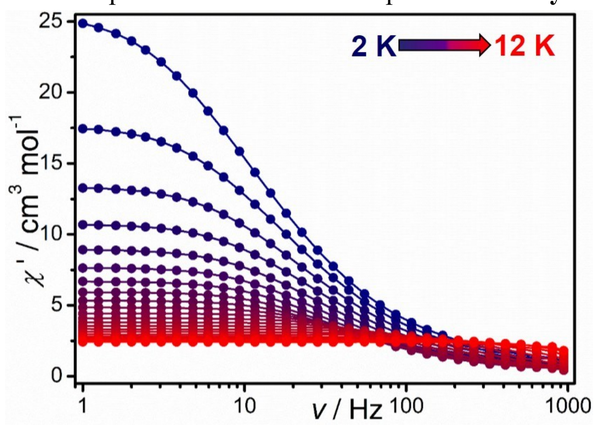

Figure S7 Frequency dependence of the in-phase (χ') ac susceptibility of **Dy** under zero dc field.

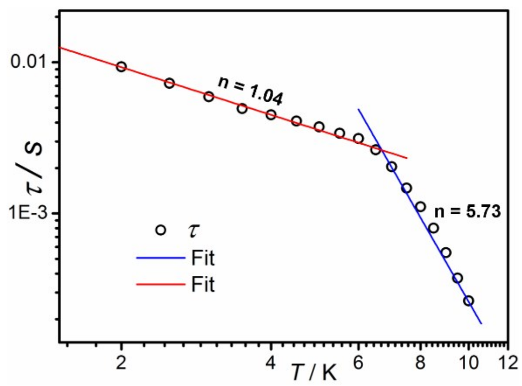

Figure S8 Plots of lnτ versus ln$T$ for **Dy** under zero dc field. The solid lines are linear fitting results.

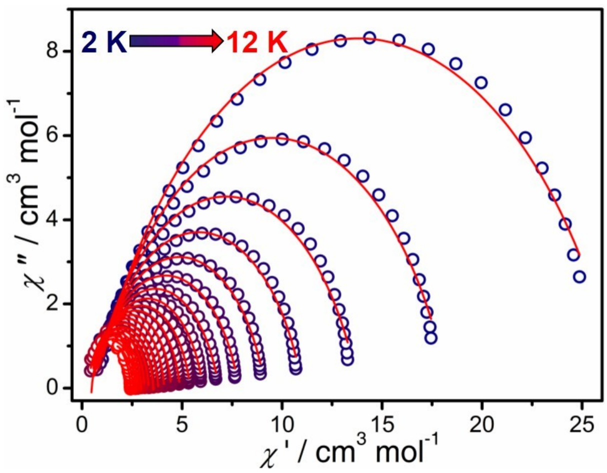

Figure S9 Cole-Cole diagram for **Dy** under zero dc field fitted by the general Debye model.

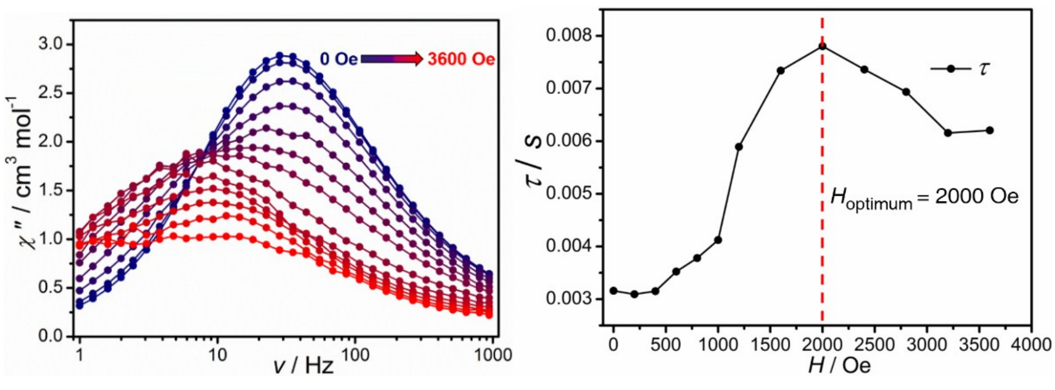

Figure S10 a) Frequency dependence of the out-of-phase (χ'') ac susceptibility for **Dy** measured at 4 K with different dc fields. b) Field dependence of the relaxation time from χ'' vs. υ data.

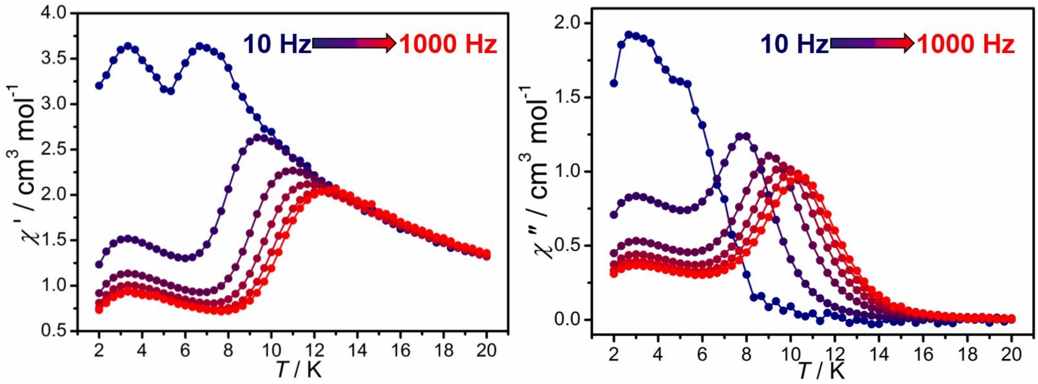

Figure S11 Temperature dependence of the in-phase (χ') and out-of phase (χ'') ac susceptibilities of **Dy** under 2000 Oe dc field.

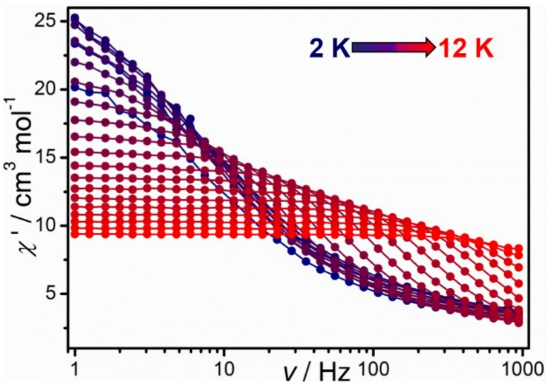

Figure S12 Frequency dependence of the in-phase (χ') ac susceptibility components of **Dy** under 2000 Oe dc field.

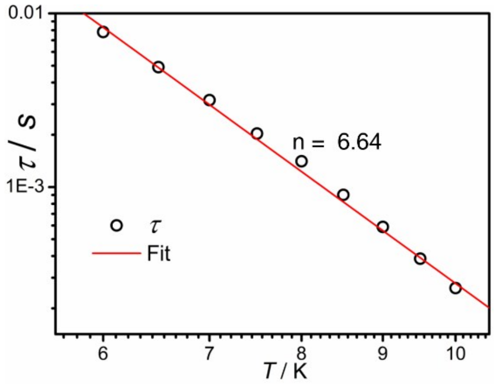

Figure S13 Plot of lnτ *versus* ln$T$ for **Dy** under 2000 Oe dc field. The solid line is linear fitting result.

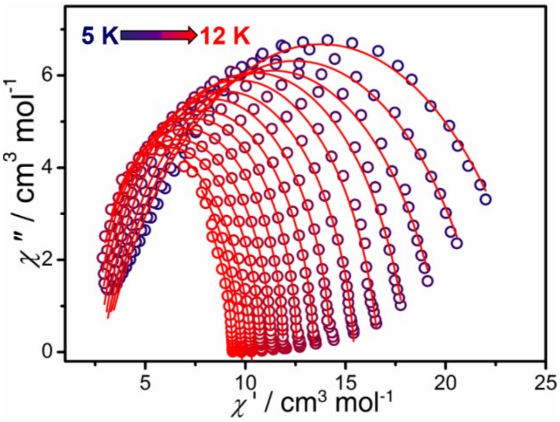

Figure S14 Cole-Cole diagram for **Dy** under 2000 Oe dc field extracted by plotting χ″ vs χ′ and fitted by the general Debye model.

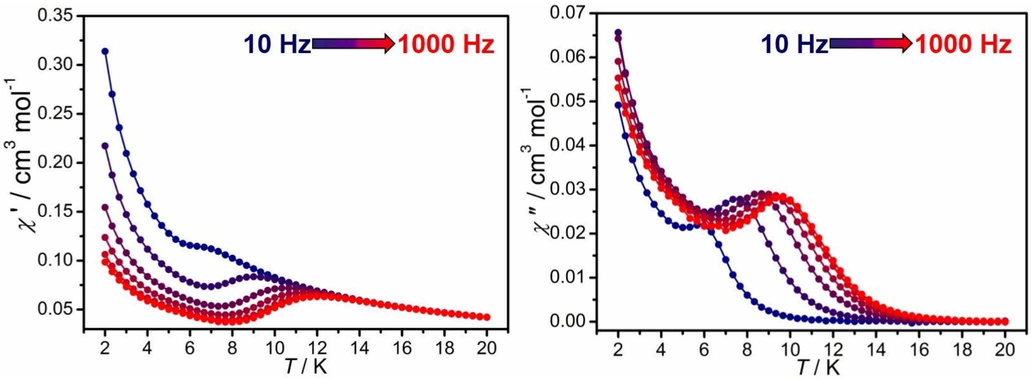

Figure S15 Temperature dependence of the in-phase (χ′) and out-of phase (χ″) ac susceptibilities of **Dy@Y** under zero dc field.

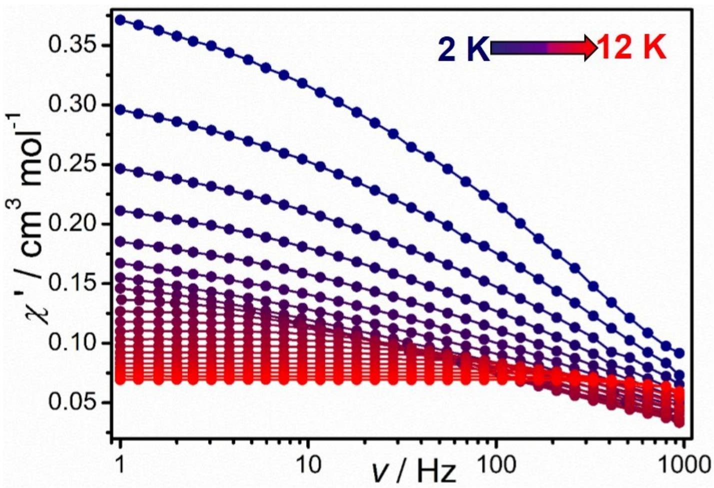

Figure S16 Frequency dependence of the in-phase (χ′) ac susceptibility of **Dy@Y** under zero dc field.

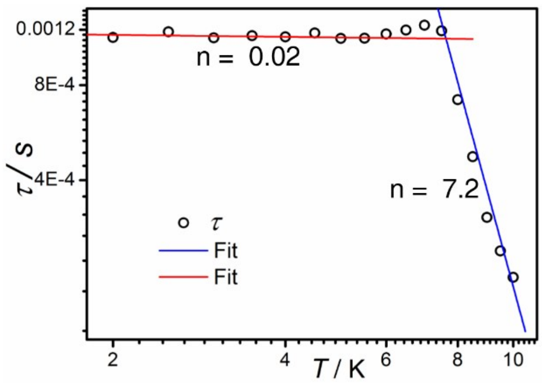

Figure S17 Plot of lnτ *versus* ln$T$ for **Dy@Y** under zero dc field. The solid line is linear fitting result.

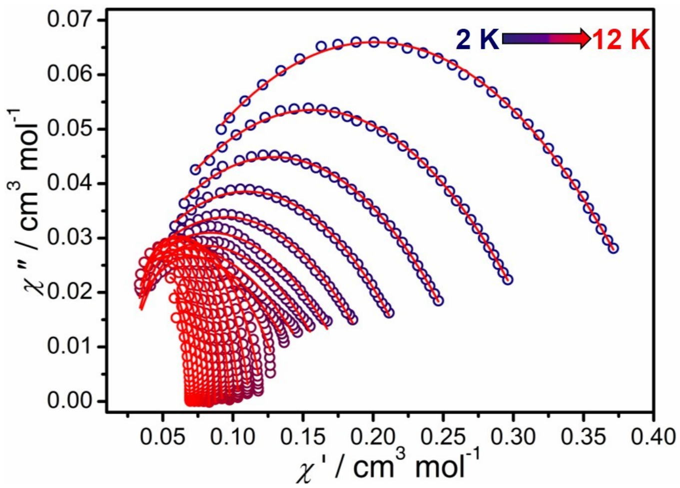

Figure S18 Cole-Cole diagram for **Dy@Y** under zero dc field fitted by the general Debye model.

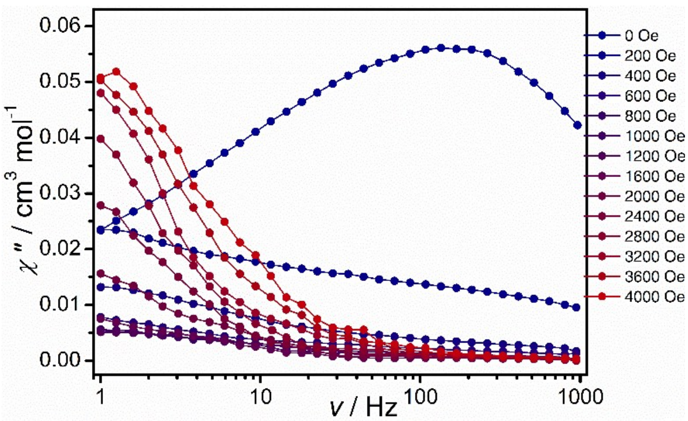

Figure S19 Frequency dependence of the out-of-phase (χ'') ac susceptibility components for **Dy@Y** measured at 2 K with different dc fields.

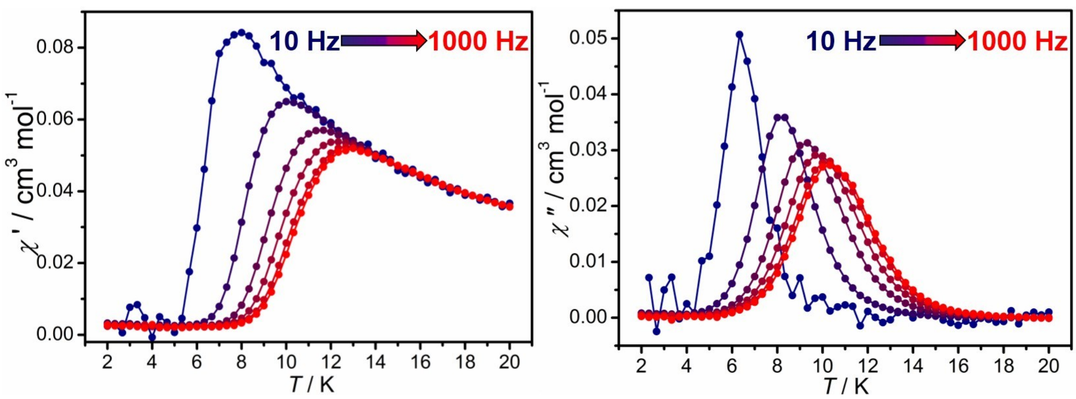

Figure S20 Temperature dependence of the in-phase (χ') and out-of phase (χ'') ac susceptibilities of **Dy@Y** under 1000 Oe dc field.

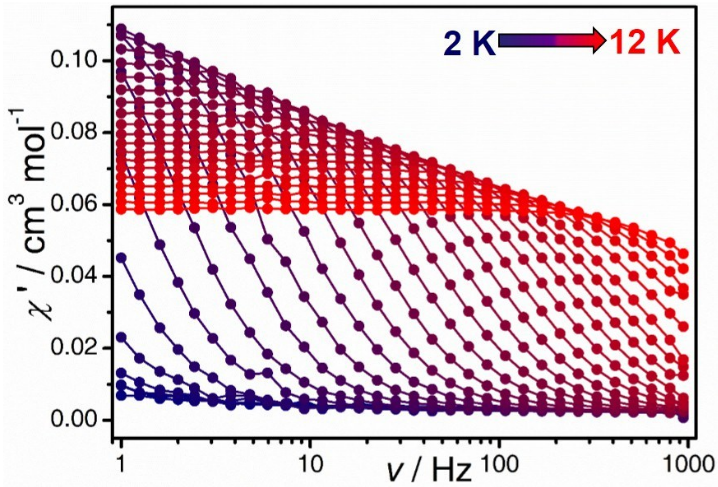

Figure S21 Frequency dependence of the in-phase (χ') ac susceptibility components of **Dy@Y** under 1000 Oe dc field.

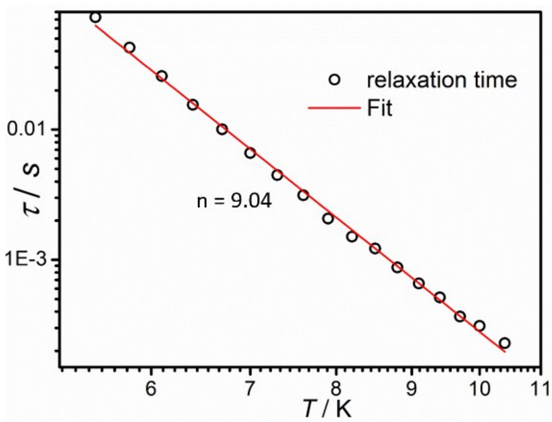

Figure S22 Plot of lnτ versus ln$T$ for **Dy@Y** under 1000 Oe dc field. The solid line is linear fitting result.

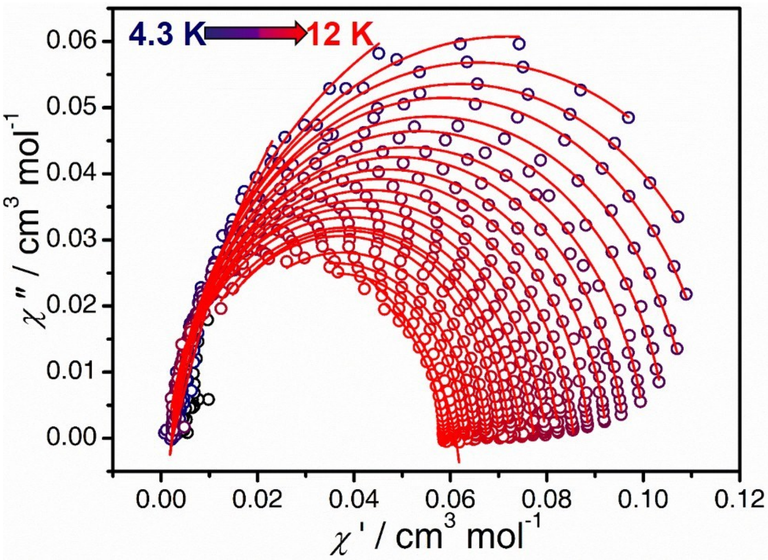

Figure S23 Cole-Cole diagram for **Dy@Y** under 1000 Oe dc field extracted by plotting χ″ vs χ′ and fitted by the general Debye model.

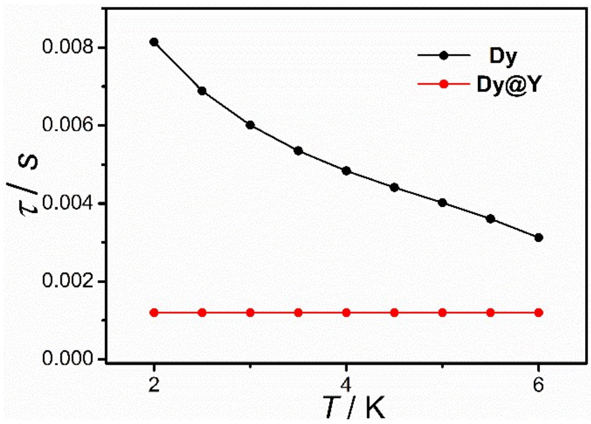

Figure S24 The relaxation time *τ* versus *T* for **Dy** and **Dy@Y** at low temperatures under zero dc field.

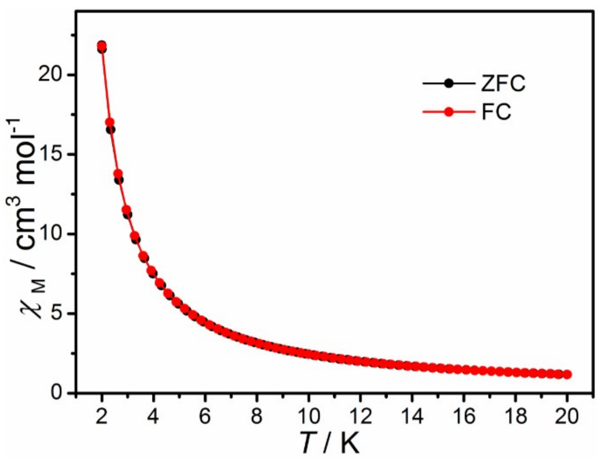

Figure S25 The ZFCM/FCM plots at 50 Oe of **Dy**.

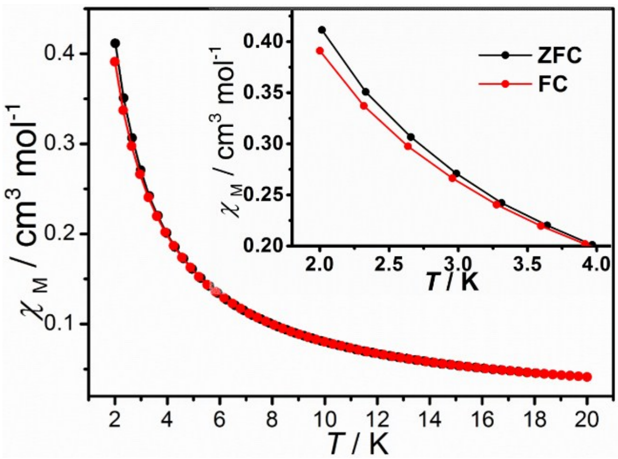

Figure S26 The ZFCM/FCM plots at 50 Oe of **Dy@Y**.

4. Tables of Magnetic Data

Table S3. The parameters of the Cole-Cole plots fitted by the general Debye models of **Dy** under zero dc field.

Dy			
T / K	χ_0	χ_1	α
2.0	0.662	26.909	0.281
2.5	0.716	18.304	0.243
3.0	0.585	13.798	0.231
3.5	0.629	11.006	0.210
4.0	0.586	9.145	0.198
4.5	0.525	7.822	0.194
5.0	0.492	6.821	0.184
5.5	0.511	6.033	0.164
6.0	0.473	5.400	0.143
6.5	0.481	4.887	0.112
7.0	0.436	4.458	0.092
7.5	0.434	4.100	0.067
8.0	0.300	3.808	0.079
8.5	0.371	3.553	0.059
9.0	0.309	3.322	0.050
9.5	0.292	3.123	0.044
10.0	0.299	2.949	0.040
10.5	0.361	2.788	0.022
11.0	0.295	2.649	0.027
11.5	0.309	3.322	0.050
12.0	0	2.411	0.037

Table S4. The parameters of the Cole-Cole plots fitted by the general Debye models of **Dy** under 2000 Oe dc field.

Dy			
T / K	χ_0	χ_1	α
5	2.904	24.668	0.299
5.5	2.862	22.091	0.259
6.0	2.836	19.936	0.210
6.5	2.800	18.120	0.148
7.0	2.698	16.645	0.106
7.5	2.566	15.442	0.082
8.0	2.478	14.258	0.045
8.5	2.300	13.431	0.038
9.0	2.293	12.574	0.009
9.5	2.143	11.887	0.003
10.0	1.866	11.294	0.013
10.5	1.514	10.758	0.025
11.0	0	10.297	0.089
11.5	0	9.810	0.083
12.0	0.091	9.354	0.028

Table S5. The parameters of the Cole-Cole plots fitted by the general Debye models of **Dy@Y** under zero dc field.

Dy@Y			
T / K	χ_0	χ_1	α
2.0	0	0.420	0.581
2.5	0	0.335	0.586
3.0	0	0.278	0.586
3.5	0	0.239	0.579
4.0	0	0.212	0.580
4.5	0	0.193	0.583
5.0	0	0.179	0.584
5.5	0	0.167	0.564
6.0	0.002	0.158	0.547
6.5	0.005	0.138	0.515
7.0	0.019	0.121	0.345
7.5	0.021	0.111	0.259
8.0	0.021	0.104	0.196
8.5	0.021	0.097	0.149
9.0	0.020	0.092	0.115
9.5	0.019	0.087	0.099
10.0	0.021	0.083	0.076
10.5	0.021	0.079	0.063
11.0	0.028	0.075	0.013
11.5	0.021	0.072	0.063
12.0	0	0.069	0.115

Table S6. The parameters of the Cole-Cole plots fitted by the general Debye models of **Dy@Y** under 1000 Oe dc field.

Dy@Y			
T / K	χ_0	χ_1	α
4.3	0.002	1.657	0.213
4.6	0.002	0.249	0.150
4.9	0.002	0.168	0.110
5.2	0.002	0.141	0.085
5.5	0.002	0.129	0.069
5.8	0.002	0.122	0.069
6.1	0.002	0.115	0.059
6.4	0.002	0.109	0.066
6.7	0.0019	0.1049	0.0654
7	0.00187	0.10052	0.0723
7.3	0.00191	0.09604	0.0642
7.6	0.00135	0.09246	0.0721
7.9	0.00189	0.08881	0.0652
8.2	0.00136	0.08558	0.0731
8.5	0.00158	0.08251	0.0731
8.8	4.63E-4	0.0798	0.0831
9.1	9.28E-4	0.0773	0.0842
9.4	0.0023	0.0747	0.0804
9.7	0.00485	0.0722	0.0444
10.0	0.00459	0.0700	0.0429
10.4	0.0077	0.0674	0.0385
10.8	0.00675	0.06518	0.06209
11.2	0.01031	0.06281	0.03329
11.6	0	0.06108	0.15572
12.0	0.00211	0.05879	0.07434